y_2'. This crossover to bicritical behavior should be especially important in the ferromagnetic regime, since it implies a change in the development of a spontaneous magnetization and a non-infinite initial susceptibility. Indeed, for $x = 0.35$, for which $g = -0.15$, crossover at $y_2' = -2$ corresponds to a temperature of 67 K, which agrees well with the observed decrease in the susceptibility for this concentration in Fig. 1. Our assertion, then, is that the drop in the ac susceptibility in the ferromagnetic phase is due not to a second-phase transition, but rather to a crossover to a bicritical behavior within that phase.

A phase diagram very similar to the one we find here has been determined by Wortis, Jayaprakash, and Riedel[3,9] from a real-space renormalization calculation of the two-δ-function model. Other models have predicted a multicritical point between spin-glass and ferromagnetic phases,[10,11] but could make no specific predictions for the exponents; here exponents are predicted for dimensions $d = 2$ and $d = 3$. As in our phase diagram (Fig. 2), the spin-glass/ferromagnetic phase boundary is found to be parallel to the temperature axis. The crossover exponent is predicted to be $\varphi = 0.72$ for $d = 2$, and $\varphi = 0.91$ for $d = 3$, bracketing our value for $\varphi = 0.77 \pm 0.05$. The exponent for the spin-glass order parameter, which is the same as that of the susceptibility at the cusp, was determined only for $d = 2$, and is $\beta_{SG} = 0.8$; our results give $\beta_{SG} = 0.50 \pm 0.08$, considerably smaller. Unfortunately, no calculation of the multicritical γ was given for any dimensionality.

The close correspondence between the phase diagram and critical exponents obtained in the position-space renormalization calculation and that of the Fe-Mn amorphous spin-glass represents the first detailed verification of any spin-glass model. We have not, of course, established the nature of the spin-glass critical line, nor determined the order parameter directly. However, the ability to perform a scaling analyses with a single crossover exponent goes far toward establishing the general picture of a multicritical point on the ferromagnetic line and a true spin-glass phase boundary for this three-dimensional random-alloy system.

We would like to thank Professor P. A. Beck for the use of his susceptibility measurement apparatus and Professor T. Rowland for assistance in this regard. This work was supported in part by National Science Foundation Grant No. DMR 78-07763 and National Science Foundation–Materials Research Laboratory Grant No. 77-23999.

[1]S. F. Edwards and P. W. Anderson, J. Phys. F 5, 965 (1976).
[2]D. Sherrington and S. Kirkpatrick, Phys. Rev. Lett. 35, 1792 (1975).
[3]M. Wortis, C. Jayaprakash, and E. K. Riedel, J. Appl. Phys. 49, 1335 (1978).
[4]H. S. Chen, R. C. Sherwood, H. J. Leamy, and E. M. Gyorgy, IEEE Trans. Mag. 12, 933 (1976).
[5]H. Gudmundsson, H. U. Åström, D. New, K. V. Rao, and H. S. Chen, to be published.
[6]H. S. Chen and C. E. Miller, Mater. Res. Bull. 11, 49 (1976).
[7]M. E. Fisher, Phys. Rev. Lett. 34, 1634 (1975).
[8]T. S. Chang, A. Hankey, and H. E. Stanley, Phys. Rev. B 8, 346 (1973).
[9]C. Jayaprakash, Ph.D. thesis, University of Illinois, 1979 (unpublished).
[10]A. B. Harris, T. C. Lubensky, and J. H. Chen, Phys. Rev. Lett. 36, 415 (1976).
[11]J. H. Chen, and T. C. Lubensky, Phys. Rev. B 16, 2106 (1977).

Exciton Dynamics within an Inhomogeneously Broadened Line

H. T. Chen and R. S. Meltzer
Department of Physics and Astronomy, University of Georgia, Athens, Georgia 30602
(Received 3 December 1979)

Exciton dynamics in $Tb(OH)_3$ is shown to depend upon the excitation location within the $k \simeq 0$ inhomoheneously broadened absorption profile. The dynamics is observed by monitoring the populations of the different k states from time-resolved band-to-band luminescence. The results indicate the presence of experimentally separable microscopic regions within which delocalized exciton states occur with well-defined k values.

Much progress in our understanding of the broadening of optical transitions in solids has been made in recent years with the advent of new laser spectroscopy techniques working in the time[1-3] and frequency domains.[4-5] For instance, fluorescence line-narrowing techniques have

made it possible to investigate the true homogeneous linewidths in solids and to examine the energy transfer process among nonresonant ions[6] by selective excitation within the inhomogeneous absorption profile.

We report here the observation of an analogous effect in which the dynamics of Frenkel excitons shows a strong dependence on the excitation location with the $k \simeq 0$ inhomogeneously broadened absorption line. The selective excitation manifests itself in the dependence of the intraband exciton scattering rate on the location of excitation within an inhomogeneously broadened absorption line. Although intraband exciton scattering has been observed in several systems,[7-9] this represents the first case in which delocalized excitons in distinct microscopic environments have been selectively prepared. The ability to selectively excite potentially large microscopic regions rather than individual sites may provide new information regarding the nature of the inhomogeneous broadening, particularly with regard to the all important question of the microscopic versus macroscopic character of the broadening.

Doubly peaked band-to-band exciton transitions,[10] shown in Fig. 1, are observed in the $({}^5D_4, \mu = 2) \rightarrow ({}^7F_5, \mu = 1)$ emission from the ferromagnet $Tb(OH)_3$. These excited states are Frenkel excitons which result from the weak exchange coupling among the $4f^8$ configurations on neighboring Tb^{3+} ions. The ${}^7F_5$, $\mu = 1$ exciton is nearly one-dimensional with predominant interactions along the c axis producing an 8-cm^{-1} dispersion while the ${}^5D_4$, $\mu = 2$ exciton has a bandwidth < 0.5 cm^{-1}. Because of its one-dimensional character and the requirement of momentum conservation in optical transitions, there is a unique correspondence between the emission wavelength and z component of the wave vector of transitions to the ${}^7F_5$, $\mu = 1$ state as shown in Fig. 1. An optical spectrometer can therefore be utilized as a wave-vector selection device, as first described by Macfarlane and Luntz[7] for MnF_2.

When the $k \simeq 0$ ${}^5D_4$, $\mu = 2$ excitons are prepared with a relatively broadbanded tunable dye laser (bandwidth 0.7 cm^{-1}) in a magnetic field of 30 kG at 1.5 °K,[8] peak II of the emission spectrum appears immediately after excitation (< 10 ns) whereas peak I requires ~ 1 μs to reach $1/e$ of its quasiequilibrium value. During the buildup of peak I, peak II decays to a quasiequilibrium population with an identical decay time. Therefore, peak II represents emission from $k_z \simeq 0$ excitons. This determines the sign of the exciton dispersions which are indicated in the energy dispersion curves in Fig. 1.

Over a fairly broad range in temperature and magnetic field (e.g., 5–20 K at 30 kG), the rate of scattering out of the $k \simeq 0$ states is proportional to the density of spin excitations in the Tb^{3+} ground-state spin system. At higher temperatures, exciton-phonon scattering dominates. However, below 5 K in a field of 30 kG, the scattering rate becomes independent of temperature and is therefore limited to impurity and defect scattering. The experiments described here were performed in a field of 30 kG and temperature of 1.5 °K and refer exclusively to impurity and defect scattering.

We now prepare the ${}^5D_4$, $\mu = 2$ excitons at $k \simeq 0$ with a 0.1-cm^{-1}-bandwidth, N_2-pumped, pulsed, tunable dye laser tuned to the resonance from the ground state at $\lambda = 4879$ Å. Time-resolved spectra are obtained for excitation at different locations within the absorption line shape, as shown in Fig. 2. When the excitons are prepared at a position 0.59 cm^{-1} on the high-energy side of the line center, only peak II appears in emission during the first 200 ns as shown in Fig. 2(a). A spectrum taken 30 μs later [Fig. 2(b)] shows the presence of all excitons, but the system has

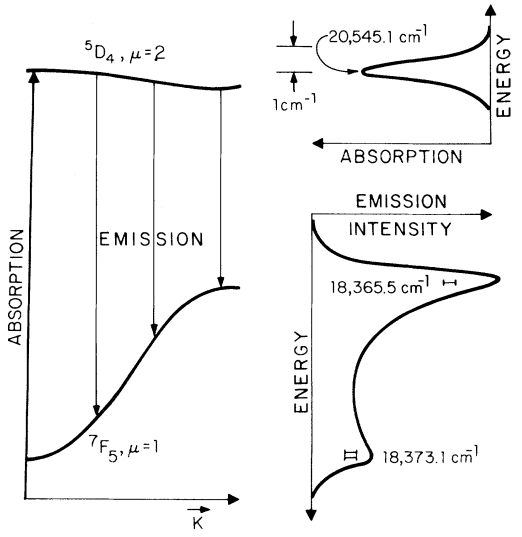

FIG. 1. One-dimensional ($\vec{k} \| c$) dispersion curves and absorption and emission line shapes for $Tb(OH)_3$ at 1.5 °K and in a 30-kG magnetic field along the c axis. Absorption is from the ground state to the $k \simeq 0$ component of the ${}^5D_4$, $\mu = 2$ state. Band-to-band emission between ${}^5D_4$, $\mu = 2$ and ${}^7F_5$, $\mu = 1$ occurs vertically at all k values and its intensity is proportional to the population of the different ${}^5D_4$ k states.

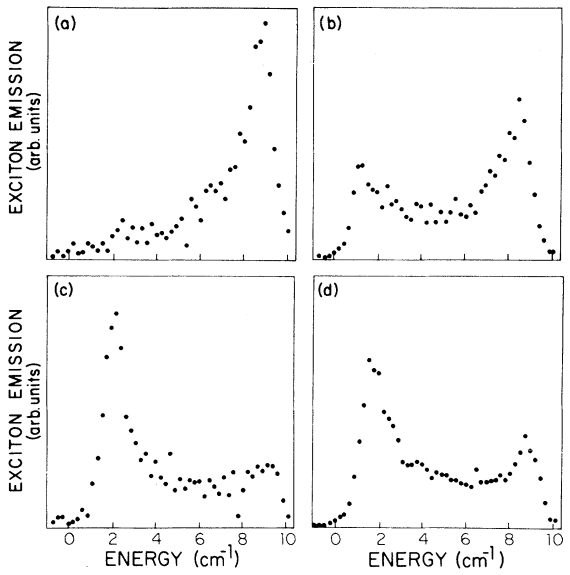

FIG. 2. (a), (b) Time-resolved band-to-band emission spectra obtained with excitation 0.59 cm^{-1} above the $^5D_4$, $\mu = 2$ absorption peak (a) averaged over the first 200 ns and (b) at 30 μs. (c),(d) Spectra obtained for excitation 0.58 cm^{-1} below the absorption peak, (c) averaged over the first 200 ns and (d) at 30 μs. The origin of the energy axis is 18 364 cm^{-1}.

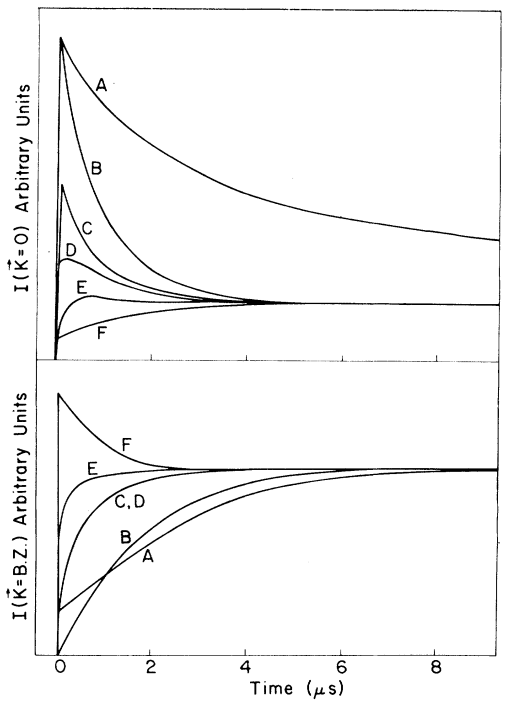

FIG. 3. Time-resolved populations of the $k \simeq 0$ and $k_z \simeq \pi/c$ (Brillouin zone) $^5D_4$, $\mu = 2$ excitons after excitation of the $k \simeq 0$ excitons for different locations within the inhomogeneous absorption profile. The excitation location relative to the peak of the absorption (in cm^{-1}) is, for curve A, 0.39; B, 0.19; C, 0.15; D, -0.08; E, -0.19; and F, -0.44.

still not reached a state of thermal equilibrium as determined by a comparison to the cw emission spectrum of Fig. 1.

However, when the $k \simeq 0$ excitons are prepared by excitation into the low-energy side of the absorption profile ($\Delta E = -0.58$ cm^{-1}), as shown in Fig. 2(c), all excitons are present in a spectrum averaged over the first 200 ns. Note that the emission line shape is not thermalized as indicated by an excess of peak I ($k_z \simeq \pi/c$) as compared with the cw spectrum in Fig. 1. However, by 30 μs the exciton distribution, shown in Fig. 2(d), is thermalized.

The effect of tuning the excitation in small increments across the absorption profile is illustrated in Fig. 3 where we show the time-resolved emission intensities observed with the spectrometer sitting on peak II ($k_z \simeq 0$) and with the spectrometer sitting on peak I ($k_z \simeq \pi/c$). In both cases, our spectral resolution is about 1 cm^{-1}. Curves A–E, covering the excitation range from $\Delta E = +0.39$ cm^{-1} to $\Delta E = -0.19$ cm^{-1}, show an initial decay of the $k_z \simeq 0$ excitons and buildup of $k_z \simeq \pi/c$ excitons with a decay rate which varies from about 5×10^6/s to 2×10^5/s over the tuning range, a variation of over an order of magnitude. Curve F, obtained for excitation at $\Delta E = -0.44$ cm^{-1}, shows quite a different behavior. Within the first 10 ns, there is a buildup of both $k_z \simeq 0$ and $k_z \simeq \pi/c$ excitons, followed by a further buildup of $k_z \simeq 0$ excitons and decay of $k_z \simeq \pi/c$ excitons at a rate of about 10^6/s.

This dependence of the exciton dynamics on location within the absorption line shape clearly indicates that the absorption is inhomogeneously broadened. More important, it means that we are able to selectively excite different regions within the sample. The nature of these regions has a strong influence on the exciton dynamics whose rates can very by orders of magnitude as the excitation is tuned by < 1 cm^{-1} across the absorption line. As the dynamics shows an energy selectively $\lesssim 0.1$ cm^{-1}, it follows that the homogeneous linewidths are less than this value, yielding an exciton coherence time > 50 ps.

Excitons created in the high-energy absorption tail (curves A and B of Fig. 3) exhibit the slowest scattering rates indicating that they exist in regions most nearly free of impurities or defects.

In addition, these excitons are delocalized with well-defined k values since emission during the first 20 ns after excitation shows the dominance of $k \simeq 0$ excitons (peak II) which, according to the optical selection rules, are the only ones which can be prepared in excitation from the ground state.

As one lowers the excitation energy, the $k \simeq 0$ exciton becomes more rapidly thermalized as indicated by the reduced relaxation times shown in Fig. 3 for curves A–E, indicating that the presence of defects or impurities generally leads to a reduction in the $^5D_4$, $\mu = 2$ exciton energy.

Under excitation in the low-energy tail, emission over the whole band appears within the first 200 ns [Fig. 2(c)], but shows a preponderance of peak I ($\vec{k}_z \simeq \pi/c$). As seen in Fig. 3 for curve F, peak I appears within the first 10 ns. We suggest that at this location within the absorption profile localized excitons are prepared which then rapidly (<10 ns) delocalize into exciton states predominantly at the zone boundary. The preference for the zone boundary may be explained by the sign of the dispersion of the $^5D_4$, $\mu = 2$ exciton band which results in $k_z \simeq \pi/c$ excitons lying at the bottom of the band, in resonance with the localized states excited in the low-energy tail of the absorption. Energy transfer from localized exciton states to delocalized $k_z \simeq \pi/c$ states in the band is strongly favored by the resonance which makes it possible for energy transfer to occur without the need of phonons to take up the energy mismatch. Further relaxation now occurs by scattering within the exciton band leading to thermal equilibrium in ~2 μs.

Our model of the $^5D_4$, $\mu = 2$ exciton states of the Tb^{3+} ion in $Tb(OH)_3$ consists of microscopic regions in which well-defined excitons can propagate. These regions are distinct from one another. A correlation exists between the $k \simeq 0$ exciton energy and the exciton dynamics within the region.

We assume that the exciton bands found in these different regions have similar dispersion curves but are shifted relative to one another by the nature of the impurities or defects within or at the edges of these regions. In regions with the lowest exciton energies, there exist Tb^{3+} ions which give rise to localized excitons whose energies are in near resonance with the $k_z \simeq \pi/c$ delocalized excitons in that region or in spatially adjacent regions.

Three important questions remain unanswered: (1) What is the nature of the impurities and defects which distinguish these regions? (2) What are the sizes of these regions? (3) Does energy transfer among different regions occur with sufficient probability to allow long-range energy migration? Since these crystals are hard to grow, it will be difficult to produce a sufficient number of well-controlled samples to answer (1). However, several experiments could provide information regarding (2) and (3). Fluorescence line-narrowing experiments with nanosecond or microsecond resolution would enable us to observe energy transport among energetically distinct regions. Transient-grating experiments[11] would indicate whether long-range energy migration occurs. These two experiments, taken together, could potentially provide information about the size of these regions, their spatial distribution, and energy migration among these regions.

We acknowledge the helpful comments of R. M. Macfarlane. This work was supported in part by the National Science Foundation and the U. S. Army Research Office, Durham.

[1]N. A. Kurnit, I. D. Abella, and S. R. Hartmann, Phys. Rev. Lett. 13, 567 (1964).

[2]A. Z. Genack, R. M. Macfarlane, and R. G. Brewer, Phys. Rev. Lett. 37, 1078 (1976).

[3]R. G. DeVoe, A. Szabo, S. C. Rand, and R. G. Brewer, Phys. Rev. Lett. 42, 1560 (1979).

[4]A. Szabo, Phys. Rev. Lett. 25, 924 (1970).

[5]A. Szabo, Phys. Rev. B 11, 4512 (1975).

[6]P. M. Selzer, D. L. Huber, B. B. Barnett, and W. M. Yen, Phys. Rev. B 17, 4979 (1978).

[7]R. M. Macfarlane and A. C. Luntz, Phys. Rev. Lett. 31, 832 (1973).

[8]R. S. Meltzer and R. L. Cone, J. Lumin. 12/13, 247 (1976); R. S. Meltzer, Solid State Commun. 20, 553 (1976).

[9]D. D. Smith and A. H. Zewail, J. Chem. Phys. 71, 3533 (1979).

[10]R. L. Cone and R. S. Meltzer, J. Chem. Phys. 62, 3573 (1975).

[11]J. R. Salcedo, A. E. Siegmann, D. D. Dlott, and M. D. Fayer, Phys. Rev. Lett. 41, 131 (1978).